Raman-active modes of porous gallium phosphide at high pressures and low temperatures

Raman-active modes of porous gallium phosphide at high pressures and low temperatures

V V Ursaki[1,2]**, F J Manjón**[1,3,6]**, K Syassen**[1]**, I M Tiginyanu**[2,4]**, G Irmer**[5]
and J Monecke[5]

[1] Max-Planck Institut für Festkörperforschung, Heisenbergstrasse 1, 70569 Stuttgart, Germany
[2] Institute of Applied Physics, Academy of Sciences of Moldova, 2028 Chisinau, Moldova
[3] Departament de Física Aplicada, Universitat Politècnica de València, EPSA, 03801 Alcoi, Spain
[4] Laboratory of Low-Dimensional Semiconductor Structures, Technical University of Moldova,
2004 Chisinau, Moldova
[5] Institut für Theoretische Physik, TU Bergakademie Freiberg, Bernhard-von-Cotta-Strasse 4,
D-09596 Freiberg, Germany

E-mail: fjmanjon@fis.upv.es

Abstract

Porous gallium phosphide (GaP) with a honeycomb-like morphology and a
skeleton relative volume concentration $c = 0.7$ was investigated by Raman
spectroscopy under pressure up to 10 GPa at $T = 5$ K. The porous samples
were prepared by electrochemical etching. The transverse optical (TO) and
longitudinal optical (LO) mode frequencies were found to shift with pressure
similarly to those of bulk GaP. As in bulk GaP, the TO feature of the porous
GaP exhibits a pressure-induced narrowing which is interpreted in terms of a
Fermi resonance. The scattering intensity observed on the low-frequency side
of the LO mode is attributed to surface-related Fröhlich mode scattering. The
latter results are interpreted on the basis of an effective medium expression for
the dielectric function. The Raman spectra indicate that both the morphology
and degree of porosity are unaffected by pressure in the range investigated.

(Some figures in this article are in colour only in the electronic version)

1. Introduction

Porous III–V compounds have recently attracted interest [1–5] due to their potential
applications in electronics and photonics [6]. By changing the morphology and characteristic
dimensions of the porous skeleton entities, the material properties can be modified in a
controlled manner. When the characteristic dimensions are smaller than the exciton Bohr

---

[6] Author to whom any correspondence should be addressed.

radius, the quantum size effects cause an increase of the band gap and strong modifications of the optical and electrical properties. Considerable changes in the optical properties of porous materials are also expected if the characteristic dimensions are much larger than the exciton Bohr radius. For instance, when electromagnetic radiation with a wavelength larger than the pore dimensions propagates through a porous structure of a polar material, the electric-field-induced polarization of the skeleton entities results in the excitation of electric dipoles vibrating at specific frequencies. These vibrations, not present in the bulk material, give rise to optical modes in Raman scattering, located in the frequency gap between the bulk transverse optical (TO) and longitudinal optical (LO) phonons of the binary compound. The surface-related optical modes, predicted by Fröhlich [7], have been calculated for small ionic crystals of different morphology by Fuchs and Kliewer [8, 9] and have been observed in infrared (IR) spectra of powders by many authors.

Fröhlich-type surface modes in mesoporous samples can be measured more easily in IR absorption and reflectance spectra than in Raman scattering because typical wavelengths in the IR experiments are much larger than the laser wavelengths commonly used in Raman spectroscopy. According to Ruppin [10], only porous gallium phosphide (GaP) samples with a crystallite size smaller than 100 nm are candidates for use in the study of the Fröhlich modes by Raman spectroscopy. Under such conditions, the scattering efficiency of the lowest-energy Fröhlich mode ($l = 0$) is comparable with those of bulk LO and TO phonons, the contributions of Fröhlich modes with $l > 0$ being negligible.

Porous GaP layers and free-standing membranes, in addition to powders, were used in investigations of Fröhlich mode behaviour [11–15]. Several theoretical calculations of these modes have dealt with the case of isolated particles [7–10]. In porous layers and free-standing membranes, a suitable effective medium expression for the dielectric function needs to be taken into account. Effective medium calculations [15–18] predict a longitudinal–transverse splitting of the Fröhlich mode. This splitting in a porous polar material was first observed by Danishevskii *et al* [19] and by Macmillan *et al* [20] in the IR reflectance spectra of porous 6H-SiC layers.

The study of porous materials under hydrostatic pressure is expected to provide additional insight into the properties of the skeleton entities. In a recent pressure Raman study [12] of porous GaP at 300 K, a rather broad feature located between the TO and LO modes was observed and attributed to Fröhlich surface scattering. A longitudinal–transverse splitting of the Fröhlich mode could not be detected in that work, but was observed in low-temperature Raman measurements at ambient pressure [21].

In this work we report Raman spectra for porous GaP measured at low temperature and under high hydrostatic pressures. We have obtained the pressure dependences of the bulk-like TO and LO mode frequencies and the corresponding Raman line as well as the frequencies of surface-related modes. Our results for the bulk-like phonons are compared with recently reported experimental and theoretical results for bulk GaP, and our results for the Fröhlich modes are compared with previous experimental results on porous samples and with a simulation based on an effective medium expression for the dielectric function.

2. Experimental details

The 30 μm thick porous membranes used in the present study were prepared on (100)-oriented Te-doped liquid-encapsulation-Czochralski-grown GaP substrates with a free electron concentration $n = 5 \times 10^{17}$ cm^{-3} at 300 K. The porosity was introduced by etching the samples for 30 min in a 0.5 molar aqueous solution of sulfuric acid at a current density 5 mA cm^{-2} using a conventional electrochemical cell with a Pt working electrode. According

to scanning electron microscope images and IR reflectance measurements [15], the membranes exhibit a honeycomb-like morphology with quasi-uniformly distributed nearly cylindrical pores stretching into the sample perpendicular to the initial crystal surface. The skeleton relative volume concentration c of different samples was estimated to vary between 0.4 and 0.7.

Raman experiments under hydrostatic pressure up to 10 GPa were performed in a backscattering geometry at $T = 5$ K using a diamond anvil cell with helium as the pressure-transmitting medium. The ruby luminescence method was used for pressure calibration [22, 23] with temperature correction according to [24]. In order to avoid non-hydrostatic conditions the pressure was changed at a temperature above the helium melting line, and this was followed by slow cooling again. Spectra with 1 cm^{-1} resolution were measured using the 514 nm line of an Ar$^+$ laser and a triple-grating spectrometer (operated in subtractive-dispersion mode) combined with a multichannel CCD detector.

3. Results and discussion

Figure 1 shows low-temperature (10 K) Raman spectra of porous GaP measured near the LO phonon frequency for three different samples with c-values of 0.40, 0.55, and 0.70. Two bands labelled S1 and S2 are seen on the low-energy side of the bulk LO phonon (405.4 cm^{-1}) in all three spectra. These bands have previously been studied both experimentally [14, 15, 21] and theoretically [16–18] and they have been attributed to the split Fröhlich modes in porous GaP. The S1 mode at the higher frequency was attributed to the transverse Fröhlich mode (FTO) and the S2 mode at the lower frequency to the longitudinal Fröhlich mode (FLO).

If the S1 and S2 modes do indeed arise from the LO–TO splitting of a Fröhlich mode ($\omega_{S1} = \omega_{FTO}$; $\omega_{S2} = \omega_{FLO}$), their frequencies should be given by the maxima of Im$[\varepsilon_{eff}(\omega)]$ and Im$[-1/\varepsilon_{eff}(\omega)]$. Here $\varepsilon_{eff}(\omega)$ is the dielectric function obtained from an effective medium expression which takes into account the degree of porosity $(1 - c)$ and the morphology of the pores. The honeycomb-like structure of our samples is best described by single cylindrical pores in the limit $c \rightarrow 1$ and by GaP plates with normals randomly distributed in the layer plane in the limit $c \rightarrow 0$. An interpolation between the two limits yields the two-dimensional Maxwell-Garnett expression for the effective dielectric function [15, 25]

$$\varepsilon_{eff}(\omega) = \varepsilon(\omega) \frac{(2 - c)\varepsilon_m + c\varepsilon(\omega)}{c\varepsilon_m + (2 - c)\varepsilon(\omega)} \qquad (1)$$

where $\varepsilon(\omega)$ is the dielectric function of bulk GaP and ε_m is that of the medium filling the pores. For vanishing phonon damping, the alternating poles and zeros of $\varepsilon_{eff}(\omega)$, with a sequence $\omega_{TO}-\omega_{FLO}-\omega_{FTO}-\omega_{LO}$, give rise to four Raman features at these frequencies.

Figure 2 shows the mode frequencies for porous GaP as a function of the relative volume fraction c, as calculated from equation (1) assuming pores filled with air. The measured LO–FLO and LO–FTO splittings for the three samples of figure 1 are also indicated in figure 2. The good agreement between the experimental and calculated frequency values provides an argument in the favour of the Fröhlich nature of the S1 and S2 modes. It should be noted that the S1 and S2 bands cannot be attributed to first- or second-order bulk phonon contributions. The calculated one-phonon density of states [26] indicates that disorder-induced scattering might contribute in this region, and this effect was indeed observed in electron-irradiated GaP [27]. However, the disorder-induced anomalous features below the TO mode frequency reported in [27] are not present in our samples. Furthermore, the calculated two-phonon density of states on the low-energy side of the LO mode is negligible [28, 29].

A porous GaP sample with the relative skeleton volume concentration $c = 0.7$ was investigated under pressure. Figure 3 shows low-temperature Raman spectra of the porous
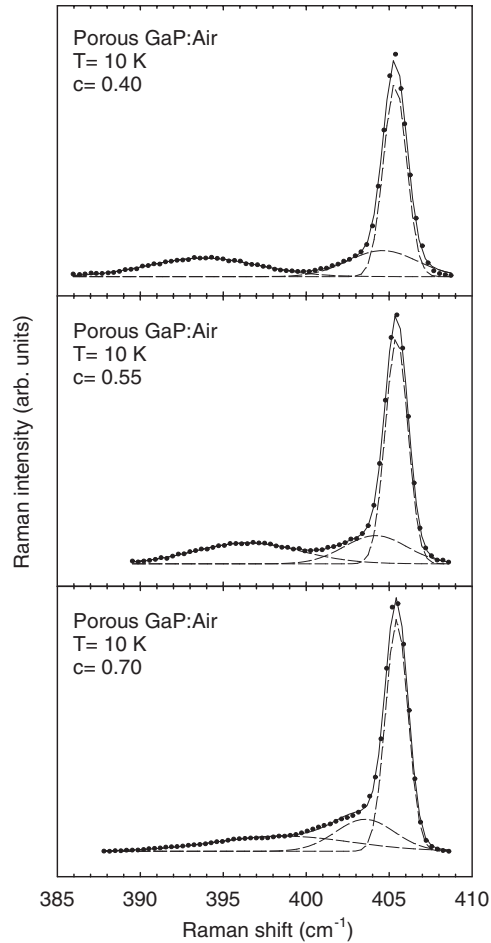
Figure 1. Low-temperature (10 K) LO Raman spectra of three porous GaP samples with different relative GaP concentrations c: (a) $c = 0.40$, (b) $c = 0.55$, and (c) $c = 0.70$. A decomposition of the spectra into three components is shown.

sample at different pressures up to 10 GPa. An increase in frequency with increasing pressure is observed for the bulk TO and LO modes and also for the S1 and S2 bands. In order to analyse the pressure behaviour of the different modes quantitatively, a spectral decomposition was used. The TO mode was modelled by a Voigt profile whereas the region near the LO mode was modelled with three Voigt profiles, as illustrated in figure 1. We note that the decomposition of the spectra near the LO mode is unique if we assume that the spectral profile consists of only three symmetric components.

Figure 4(a) shows the pressure dependences of the bulk TO and LO and the S1 and S2 mode frequencies in porous GaP at 5 K as a function of pressure, as obtained from the above decomposition. In table 1, we summarize the ambient-pressure frequencies, the pressure coefficients, and the mode Grüneisen parameters. For the calculation of the mode Grüneisen parameters, a bulk modulus of 88.2 GPa was used [30]. For comparison, we also list in table 1 the results of room temperature Raman measurements of porous GaP samples and corresponding results from a recent low-temperature study of isotopically pure single-crystal [69]GaP by Ves *et al* [31].
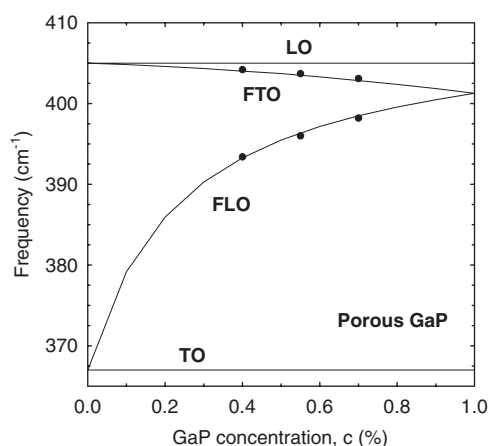
Figure 2. Calculated frequencies of the TO, LO, FTO, and FLO Raman modes as a function of the relative GaP concentration in porous GaP according to equation (1). The pores are assumed to be filled with air. Dots refer to the frequencies of the S1 and S2 features indicated in figure 1.
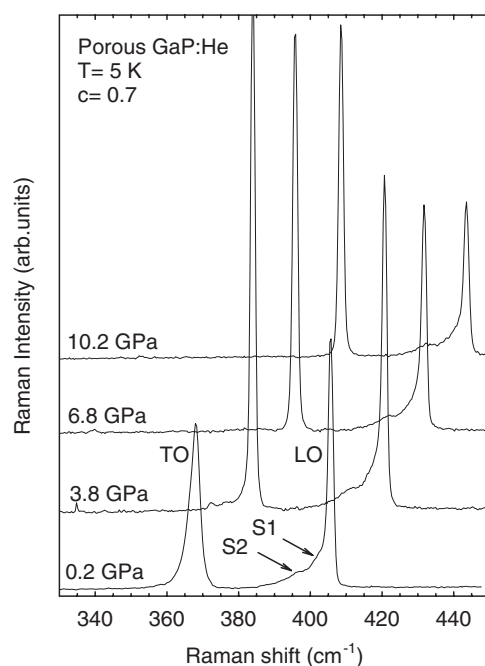
Figure 3. Low-temperature Raman spectra of porous GaP at selected pressures. The sample was immersed in helium.

Small differences in zero-pressure frequency values and linear pressure coefficients of the LO and TO modes carry limited significance, because data evaluation procedures (fits of linear or quadratic relations) differ for the different experiments. The fact that bulk ^{69}GaP exhibits slightly larger TO and LO phonon frequencies compared to the porous sample investigated here is consistent with the different isotopic compositions [28]. The shifts of TO and LO mode frequencies with pressure are nearly identical in bulk GaP and the porous material. This is
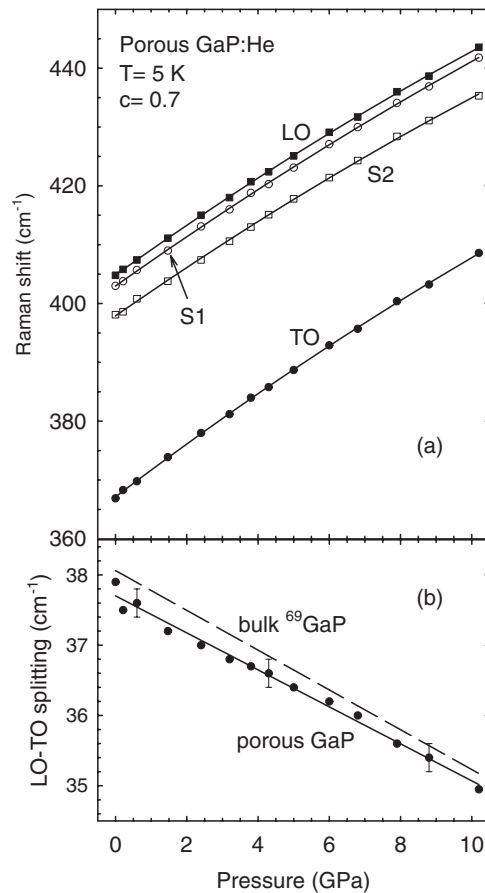
Figure 4. (a) Pressure dependences of the TO (full circles) and LO (full squares) modes and of the S1 (empty circles) and S2 (empty squares) features. The quadratic fits of the pressure dependence of the mode frequencies are also shown (solid lines). (b) The pressure dependence of the LO–TO splitting of porous GaP at 5 K (symbols) and of bulk ^{69}GaP at 10 K (dashed line, [31]). The solid line is a guide to the eye.

illustrated in figure 4(b) which shows the pressure dependence of the LO–TO splitting for our porous sample and that of bulk ^{69}GaP [31]. The LO–TO splittings decrease in the two samples at almost the same rate; this decrease in splitting is related to the reduction of the transverse effective charge under pressure.

As regards the results obtained for porous samples at low and room temperatures, the main difference is that the S1 and S2 features can be distinguished at low temperatures whereas only a single broad feature was observed at RT. Figure 5 shows the measured frequency differences between the LO and the S1 and S2 features as a function of pressure. The LO–S1 frequency difference clearly increases with increasing pressure in agreement with the previously measured behaviour of the S mode in porous GaP [12]. The observed effect of pressure on the S1–LO and S2–LO frequency differences is consistent with what would be expected on the basis of the effective medium expression (1). Assuming a pressure-independent porosity and morphology and by taking into account the pressure dependence of the dielectric constant of the helium filling the pores [32] and of the GaP skeleton [33], one obtains frequency shifts of the FLO
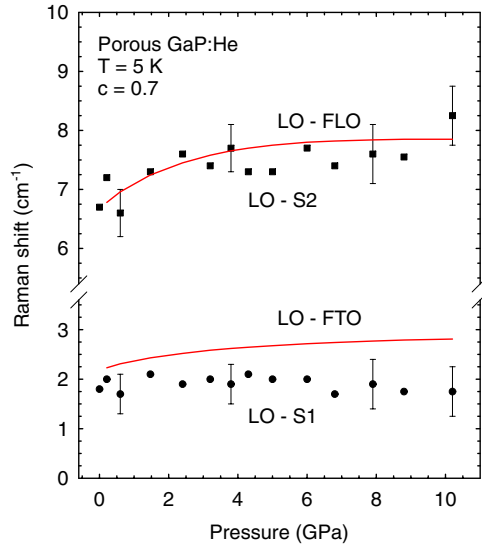
Figure 5. Frequency differences between the LO Raman mode and the S1 and S2 features as a function of pressure. Full symbols relate to experimental data. Calculations of the LO–FTO and LO–FLO frequency differences according to equation (1) are shown by solid curves. The pressure dependences of the dielectric constants of helium and GaP are taken into account and a constant porosity ($c = 0.7$) was assumed.

Table 1. Ambient-pressure frequencies ω_0 (in cm^{-1}), pressure coefficients (in cm^{-1} GPa^{-1}), and mode Grüneisen parameters for Raman modes in porous GaP with pores filled with helium. For comparison, the low-temperature data for bulk ^{69}GaP after [31] and the room temperature data for porous GaP after [12] are also listed.

Peak or mode	ω_0 (cm^{-1})	$\mathrm{d}\omega/\mathrm{d}P$ (cm^{-1} GPa^{-1})	$\mathrm{d}^2\omega/\mathrm{d}P^2$ (cm^{-1} GPa^{-2})	γ	Temperature (K)	Type of sample	Reference
TO	367.1(1)	4.59(5)	−0.053(5)	1.10(1)	5	Porous	This work
	365.8	4.43		1.07	300	Porous	[12]
	367.5	4.60		1.11	300	Bulk	[12]
	368.4	4.90		1.18	10	Bulk	[31]
FLO	397.9(2)	4.21(7)	−0.050(7)	0.93(2)	5	Porous	This work
S^a	395.5	3.78		0.85	300	Porous	[12]
FTO	403.0(1)	4.28(5)	−0.046(5)	0.94(1)	5	Porous	This work
LO	404.8(1)	4.34(4)	−0.053(4)	0.95(1)	5	Porous	This work
	402.5	3.80		0.84	300	Porous	[12]
	406.0	4.10		0.89	300	Bulk	[12]
	406.5	3.88		0.85	10	Bulk	[31]

^{a} These data correspond to the S surface mode in [12] which is supposed to be a mixture of the FTO and FLO modes.

and FTO modes shown by solid lines in figures 4(a) and 5. The results for the FLO mode agree quite well with the experimental observations. The slight disagreement for the FTO and the observed S1 feature could be due to some ambiguity in the spectral decomposition. The S1 band overlaps with the much stronger LO mode and we cannot rule out an asymmetric LO phonon broadening due to phonon confinement effects in thin skeleton wells or to a non-uniform porosity distribution in the sample. These effects could also explain the large FWHM of the FLO mode which should be much narrower according to theoretical calculations [3, 15].
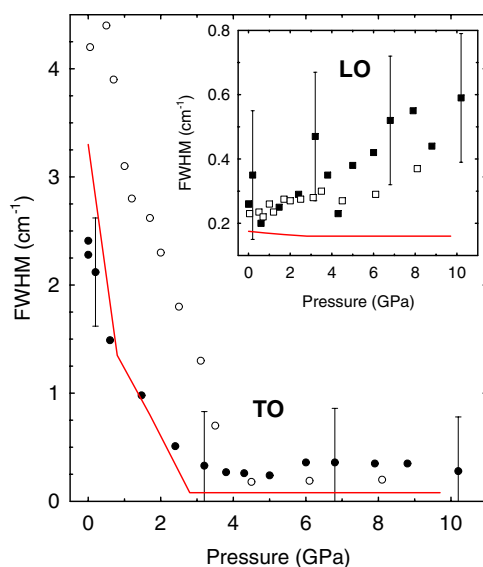
Figure 6. The FWHM for the TO and LO modes of porous GaP at 5 K as a function of pressure. The pressure dependences of the TO and LO modes in bulk ^{69}GaP [31] are shown by open symbols. Both sets of experimental data can be compared to the theoretical results (solid lines) obtained by A Debernardi in [37].

Finally, we compare the linewidths of the TO and LO modes in the porous sample with corresponding low-temperature data for bulk GaP. The TO Raman mode of bulk GaP at ambient pressure exhibits an anomalous lineshape [28, 31, 34] due to a Fermi resonance with the two-phonon density of states [35–39]. As the two-phonon density of states feature resonant in energy with the TO mode shifts with pressure at a smaller rate than the TO mode, the lineshape anomaly of the TO mode disappears with increasing pressure. This effect was observed by Weinstein [34] and Ves *et al* [31] and also predicted by theoretical calculations based on density functional perturbation theory [37].

Porous GaP exhibits a similar behaviour under pressure. Figure 6 shows the pressure dependence of the full widths at half-maximum (FWHM) of the TO and LO phonons in the porous sample after correction for the spectrometer resolution. The FWHM of the TO and LO modes measured by Ves *et al* in bulk ^{69}GaP and the theoretically predicted behaviour of the FWHM for these modes assuming natural isotopic composition [37] are also shown for comparison. The experimental results for the porous material agree very well with the predicted behaviour. This also applies to the data of Ves *et al* if the different isotopic composition of their sample is taken into account in the calculations [38]. Our results indicate that neither the porosity nor the morphology of the porous sample affect the TO and LO linewidths.

In summary, we have investigated Raman modes of porous GaP with a honeycomb-like morphology and a relative GaP skeleton volume of $c = 0.7$ as a function of pressure at low temperature. The pressure dependence of the TO and LO mode frequencies and widths of the GaP skeleton in the porous material are found to be very similar to those of bulk GaP. The effect of pressure on Raman features attributed to Fröhlich modes has been explained in terms of an effective medium expression for the dielectric function. Our results indicate that the crystalline quality of the GaP skeleton in the porous sample is similar to that of the bulk material, and that both the morphology and the degree of porosity are unaffected by pressure in the range investigated up to 10 GPa under truly hydrostatic conditions.

Acknowledgments

References

[1] Takizawa T, Arai S and Nakahara M 1994 *Japan. J. Appl. Phys.* **33** L643
[2] Erne B H, Vanmaekelbergh D and Kelly J J 1996 *J. Electrochem. Soc.* **143** 1137
[3] Tiginyanu I M, Irmer G, Monecke J and Hartnagel H L 1997 *Phys. Rev.* B **55** 6739
[4] Lockwood D J, Achmuki P, Labbe H J and Fraser J 1999 *Physica E* **4** 102
[5] Tiginyanu I M, Kravetsky I V, Monecke J, Cordts W, Marowsky G and Hartnagel H L 2000 *Appl. Phys. Lett.* **77** 2415
[6] Bell J 1999 *Opt. Laser Eur.* **60** 31
[7] Fröhlich H 1949 *Theory of Dielectrics* (Oxford: Clarendon)
[8] Fuchs R and Kliewer K L 1965 *Phys. Rev.* A **140** 2076
[9] Fuchs R and Kliewer K L 1967 *J. Opt. Soc. Am.* **58** 319
[10] Ruppin R 1975 *J. Phys. C: Solid State Phys.* **8** 1969
[11] Kuriyama K, Ushiyama K, Ohbora K, Miyamoto Y and Takeda S 1998 *Phys. Rev.* B **58** 1103
[12] Tiginyanu I M, Ursaki V V, Raptis Y S, Stergiou V, Anastassakis E, Hartnagel H L, Vogt A, Prevot B and Schwab C 1999 *Phys. Status Solidi* b **211** 281
[13] Sarua A, Tiginyanu I M, Ursaki V V, Irmer G, Monecke J and Hartnagel H L 1999 *Solid State Commun.* **112** 581
[14] Sarua A, Irmer G, Monecke J, Tiginyanu I M, Schwab C, Grob J-J and Hartnagel H L 2000 *J. Appl. Phys.* **88** 7006
[15] Sarua A, Monecke J, Irmer G, Tiginyanu I M, Gartner G and Hartnagel H L 2001 *J. Phys.: Condens. Matter* **13** 6687
[16] Monecke J 1989 *Phys. Status Solidi* b **154** 805
[17] Monecke J 1989 *Phys. Status Solidi* b **155** 437
[18] Monecke J 1994 *J. Phys.: Condens. Matter* **6** 907
[19] Danishevskii A M, Shuman V B, Rogachev A Yu and Ivanov P A 1995 *Semiconductors* **29** 1106
[20] MacMillan M F, Devaty R P, Choyke W J, Goldstein D R, Spanier J E and Kurtz A D 1996 *J. Appl. Phys.* **80** 2412
[21] Ursaki V V, Tiginyanu I M, Ricci P C, Anedda A, Foca E V and Syrbu N N 2001 *J. Phys.: Condens. Matter* **13** 4579
[22] Piermarini G J, Block S, Barnett J D and Forman R A 1975 *J. Appl. Phys.* **46** 2774
[23] Mao H K, Xu J and Bell P M 1986 *J. Geophys. Res.* **91** 4673
[24] Buchsbaum S, Mills R L and Schiferl D 1984 *J. Phys. Chem. US* **88** 2522
[25] Maxwell-Garnett J C 1904 *Phil. Trans. R. Soc.* A **203** 385
[26] Kunc K, Balkanski M and Nusimovici M A 1975 *Phys. Status Solidi* b **72** 229
[27] Azhniuk Yu M, Gomonnai A V, Goyer D B, Megela I G, Kranjcec M and Lopushansky V V 2001 *Phys. Status Solidi* b **227** 595
[28] Widulle F, Ruf T, Göbel A, Schönherr E and Cardona M 1999 *Phys. Rev. Lett.* **82** 5281
[29] Kunc K 1973–1974 *Ann. Phys., Paris* **8** 319
[30] Madelung O and Schulz M (ed) 1987 *Landolt–Börnstein New Series* Group III, vol 22 (Berlin: Springer)
[31] Ves S, Loa I, Syassen K, Widulle F and Cardona M 2001 *Phys. Status Solidi* b **223** 241
[32] Toullec R L, Loubeyre P and Pinceaux J P 1989 *Phys. Rev.* B **40** 2368
[33] Strössner K, Ves S and Cardona M 1985 *Phys. Rev.* B **32** 5514
[34] Weinstein B A 1976 *Solid State Commun.* **20** 999
[35] Krauzman M, Pick R M, Poulet H, Hamel G and Prevot B 1974 *Phys. Rev. Lett.* **33** 528
[36] Kanellis G, Kress W and Bilz H 1986 *Phys. Rev. Lett.* **56** 938
[37] Debernardi A 2000 *Solid State Commun.* **113** 1
[38] Debernardi A 2002 *Physica* B **316/317** 35
[39] Menéndez J and Cardona M 1984 *Phys. Rev.* B **29** 2051